TABLE VI. Equivalent tube length ΔL.

ρ_0	Disk	Oblate	Sphere	Prolate
$0.1a$	$0.000849a$	$0.001411a$	$0.002002a$	$0.003231a$
$0.2a$	$0.006809a$	$0.011332a$	$0.016107a$	$0.026073a$
$0.3a$	$0.023135a$	$0.038670a$	$0.055187a$	$0.09002a$
$0.4a$	$0.05559a$	$0.093740a$	$0.134879a$	$0.22277a$
$0.5a$	$0.11124a$	$0.19044a$	$0.27767a$	$0.4664a$
$0.6a$	$0.2002a$	$0.35104a$	$0.52205a$	$0.895a$
$0.7a$	$0.34a$	$0.618a$	$0.94634a$	$1.7a$
$0.8a$	$0.5a$	$1.10a$	$1.75124a$	...
$0.9a$	...	$2.1a$	$3.7277a$	...
$0.95a$	...	$3.a$	$6.6207a$	...

is applied to the line integral of (5), the result is zero so the spheroid vortices contribute nothing. The same operations, performed after substitution of $-K_1(ta)I_1(t\rho)/I_1(ta)$ for $K_1(t\rho)$ give zero except when $n = 0$ so that the contribution of the wall vortices, for all spheroids, is

$$\Delta L = v_0^{-1} \int_{-\infty}^{\infty} v_z \, dz = \tfrac{1}{3}(2\rho_0/a)^2 C_0^2 c. \qquad (23)$$

This also gives the resistance increase of a solid conducting cylinder due to the presence of a coaxial nonconducting spheroid inside it in terms of the equivalent additional cylinder length. The specific formulas for the cases treated are

$$\begin{aligned} &\text{Sphere and disk} && \Delta L = 4\rho_0^3 C_0/(3a^2), \\ &\text{Oblate (2 to 1)} && \Delta L = 2\rho_0^3 C_0/(3^{\frac{1}{2}}a^2), \\ &\text{Prolate (1 to 2)} && \Delta L = 4\rho_0^3 C_0/(3^{\frac{1}{2}}a^2). \end{aligned} \qquad (24)$$

The results appear in Table VI. Unfortunately C_0 is so poorly determined in some cases, for reasons already mentioned, that ΔL cannot be found. It is probable, but not certain, that all the digits in Table VI are significant.

THE PHYSICS OF FLUIDS VOLUME 7, NUMBER 5 MAY 1964

Hydraulic Jump in a Rotating Fluid

CHIA-SHUN YIH, H. E. GASCOIGNE, AND W. R. DEBLER
Department of Engineering Mechanics, University of Michigan, Ann Arbor, Michigan
(Received 18 March 1963; revised manuscript received 29 November 1963)

A hydraulic jump occurs in a layer of fluid flowing down the inner wall of a rotating cylinder when the downstream conditions are adequate. The theory of these jumps is presented, together with supporting experimental data. The results confirm the similarity between free-surface flows under general rotation (and hence centripetal acceleration) and free-surface flows in the presence of a gravitational field, and indicate that the hydraulic jump in a rotating fluid is just the counterpart of the ordinary hydraulic jump.

1. INTRODUCTION

IT has been generally recognized that the flows of a rotating fluid are, in many respects, similar to the flows of a stratified fluid in the presence of a gravitational field. Since a free surface is a surface of density discontinuity, which is a form of extreme stratification, there is also a similarity of flows of a rotating fluid with a free surface to free-surface flows in the gravitational field. A free surface in the rotating fluid is necessary to ensure similarity of its flow to a free-surface flow in the gravitational field because the quantity corresponding to a discontinuity in specific weight in the latter is a discontinuity in $\rho\Gamma^2$ in the former, ρ being the density and Γ the circulation of the flow along any circle in its domain located with axial symmetry. Thus the counterpart of the ordinary hydraulic jump appears to be a hydraulic jump in a layer of liquid flowing down the inner wall of a rotating cylinder, and rotating with it. The analytical and experimental results are presented in this paper to provide yet another instance of the similarity of rotating flows and stratified flows.

The hydraulic jump in a swirling fluid has also been observed by Binnie.[1] But the tube he used was stationary, and his work was not primarily a study of the jump.

2. ANALYSIS

With reference to Fig. 1, b is the inner radius of the tube, d_1 is the depth of water upstream from

[1] A. M. Binnie, Proc. Roy. Soc. (London) **A270**, 452 (1962).

the jump, and d_2 the downstream depth. The pressure in the fluid upstream from the jump is

$$p_1 = \tfrac{1}{2}\rho\omega_1^2(r^2 - a_1^2) \qquad (\omega_1 = \omega), \tag{1}$$

in which ω_1 is the angular speed of the rotating water film, and is equal to the angular speed ω of the rotating cylinder, r is the radial distance from the axis to the point at which the pressure is being considered, and $a_1 = b - d_1$. Downstream from the jump, the angular speed ω_2 of the fluid in general varies from one radial position to another. Two extreme situations may be considered. If viscous and turbulent mixings are ignored, Kelvin's theorem on the conservation of circulation enable one to compute ω_2 as a function of r, upon utilization of the equation of continuity and the assumption that the downstream velocity U_2 is constant. This would be a very unrealistic situation, because there is violent turbulent mixing at the jump, so that Kelvin's theorem cannot be valid. The other extreme condition is the condition of complete mixing, so that after the jump another *uniform* ω_2 exists, which can be computed from ω_1 by use of the conservation of the integrated angular momentum. Thus, on the assumption that ω_2 is uniform, the downstream pressure distribution is given by

$$p_2 = \tfrac{1}{2}\rho\omega_2^2(r^2 - a_2^2), \tag{2}$$

in which $a_2 = b - d_2$. The total axial force acting at an upstream section (Section 1-1) is

$$P_1 = \int_{a_1}^{b} p_1 2\pi r\, dr = \tfrac{1}{4}\rho\pi\omega^2(b^2 - a_1^2)^2. \tag{3}$$

The total axial force acting at downstream section (Section 2-2) is

$$P_2 = \int_{a_2}^{b} p_2 2\pi r\, dr = \tfrac{1}{4}\rho\pi\omega_2^2(b^2 - a_2^2)^2. \tag{4}$$

The discharge is given by

$$Q = \int_{a_1}^{b} U_1 2\pi r\, dr = \int_{a_2}^{b} U_2 2\pi r\, dr, \tag{5}$$

which is the equation of continuity. The downstream flow is very turbulent, so that U_2 can be assumed constant without appreciable error. If the upstream flow is also turbulent, U_1 can also be assumed constant, thus the equation of continuity can be written as

$$U_1(b^2 - a_1^2) = U_2(b^2 - a_2^2). \tag{6}$$

The momentum flux through Section 1-1 is

$$M_1 = \int_{a_1}^{b} \rho U_1^2 2\pi r\, dr, \tag{7}$$

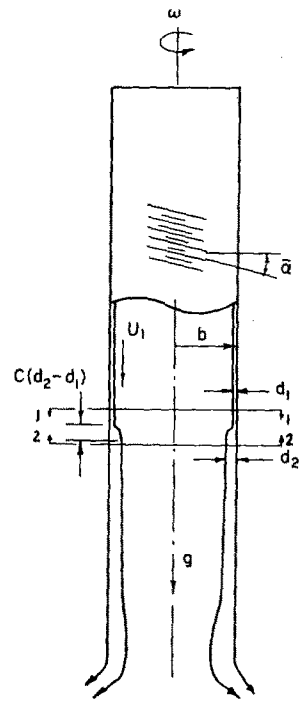

FIG. 1. Definition sketch.

and that through Section 2-2 is

$$M_2 = \int_{a_1}^{b} \rho U_2^2 2\pi r\, dr. \tag{8}$$

Since U_1 and U_2 are assumed constant,

$$M_1 = \rho\pi U_1^2(b^2 - a_1^2), \qquad M_2 = \rho\pi U_2^2(b^2 - a_2^2). \tag{9}$$

The fluxes of angular momenta are the same before and after the jump, since the torque exerted by the wall of the cylinder can be neglected. Thus

$$\int_{a_1}^{b} (\rho\omega r^2) U_1 2\pi r\, dr = \int_{a_1}^{b} (\rho\omega_2 r^2) U_2 2\pi r\, dr. \tag{10}$$

Now ω is constant, and as explained before U_1, U_2, and ω_2 can be assumed constant. Thus (10) becomes

$$\rho\omega U_1(b^4 - a_1^4) = \rho\omega_2 U_2(b^4 - a_2^4). \tag{11}$$

which can be reduced to

$$\omega(b^2 + a_1^2) = \omega_2(b^2 + a_2^2) \tag{12}$$

by the use of (6).

The momentum equation applied to the fluid between Sections 1-1 and 2-2 is

$$P_1 - P_2 + W = M_2 - M_1, \tag{13}$$

in which W is the weight of the body of fluid in the region of change of depth. If the inner radius of that body of fluid is assumed to vary linearly (with 3) from a_1 to a_2, and if the length of the jump is assumed

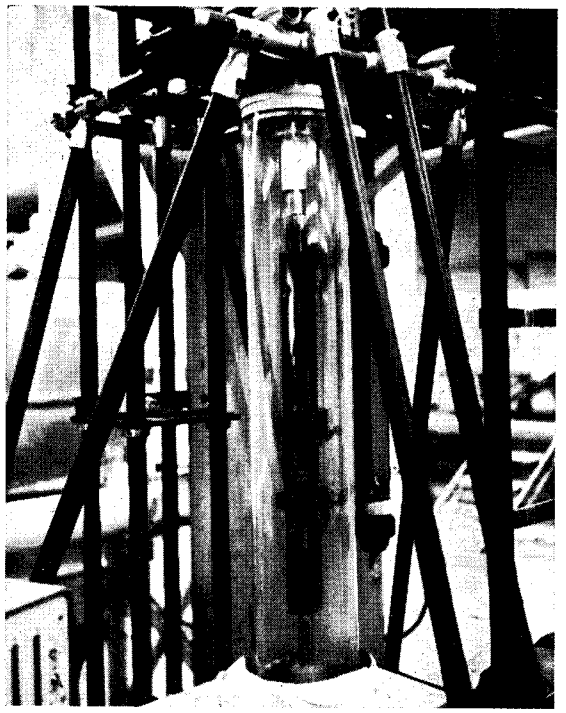

FIG. 2. A photograph of the apparatus used.

to be $c(a_1 - a_2)$, c being a constant of proportionality,

$$W = g\rho\pi(a_1 - a_2)[b^2 - \tfrac{1}{3}(a_1^2 + a_1a_2 + a_2^2)]$$
$$= g\rho\pi(a_1 - a_2)[b^2 - a_1a_2 - \tfrac{1}{3}(a_1 - a_2)^2]. \quad (14)$$

Equation (13) then becomes

$$\tfrac{1}{4}\rho\pi[\omega^2(b^2 - a_1^2)^2 - \omega_2^2(b^2 - a_2^2)]$$
$$+ g\rho\pi(a_1 - a_2)[b^2 - a_1a_2 - \tfrac{1}{3}(a_1 - a_2)^2]$$
$$= \rho\pi[U_2^2(b^2 - a_2^2) - U_1^2(b^2 - a_1^2)]. \quad (15)$$

Now if (6) is used on the right-hand side, (12) is used to eliminate ω_2 and for simplicity one writes

$$\alpha_1 = \frac{a_1}{b}, \qquad \alpha_2 = \frac{a_2}{b}, \qquad F_1 = \frac{U_1}{\omega b}, \qquad G = \frac{g}{b\omega^2}.$$

One obtains, after simplifications,

$$(1 - \alpha_1^2\alpha_2^2)(1 - \alpha_2^2) = F_1^2(1 - \alpha_1^2)(1 + \alpha_2^2)$$
$$+ \frac{cG(1 - \alpha_2^2)(1 + \alpha_2^2)^2[3(1 - \alpha_1\alpha_2) - (\alpha_1 - \alpha_2)^2]}{3(\alpha_1 + \alpha_2)}. \quad (16)$$

This equation enables one to find α_2 for given values of α_1, F_1, G, and c.

In the experiments performed, d_1 and d_2 were very small compared with b. Hence a_1 and a_2 were nearly equal to b and so α_1 and α_2 were nearly equal to 1. Putting α_1 and α_2 equal to 1 except where differences are involved, one obtains from (16)

$$(1 - \alpha_1\alpha_2)(1 - \alpha_2) = 2F_1^2(1 - \alpha_1)$$
$$+ cG(1 - \alpha_2)[(1 - \alpha_1\alpha_2) - \tfrac{1}{3}(\alpha_1 - \alpha_2)^2]. \quad (17)$$

Now with

$$\eta = d_2/d_1 \quad \text{and} \quad F^2 = U^2/\omega^2 b d_1$$

one has

$$1 - \alpha_1\alpha_2 = (d_1/b)(1 + \eta), \quad (1 - \alpha_2) = (d_1/b)\eta,$$
$$F_1^2(1 - \alpha_1) = F_1^2(d_1/b)$$

and

$$(\alpha_1 - \alpha_2)^2 = (d_1^2/b^2)(\eta - 1)^2.$$

Thus (17) can be written as

$$\eta(\eta + 1)(1 - cG) + \tfrac{1}{3}\frac{d_1}{b}cG\eta(\eta - 1)^2 = 2F^2. \quad (18)$$

The depth ratio η had a maximum value of 10.7 in one test, and less than 10 on all the other tests, and d_1/b was very small. Thus, under the experimental conditions, the second term on the right-hand side can be neglected. The resulting equation can be solved simply. The solution is

$$\eta = \frac{d_2}{d_1} = \frac{1}{2}\left[-1 + \left(1 + \frac{8F^2}{1 - cG}\right)^{\frac{1}{2}}\right]. \quad (19)$$

Equations (17) and (18) are identical in substance,

FIG. 3. A photograph showing location of the jump and streaks in the flow.

and are approximations to (16). Equation (16) corresponds to the momentum equation in ordinary hydraulic-jump theory, except that the weight of the fluid in the region of variable depth plays a part here, but not in the ordinary hydraulic jump.

3. APPARATUS AND METHOD OF MEASUREMENT

The apparatus is shown in Fig. 2. The working section was a piece of transparent tube of polished cast resin about 50 in. long and 9 in. o.d. The wall was $\frac{1}{4}$ in. thick. The innersurface diameter had a variation of at most 0.012 in. The tube is supported by a rigid hub at the top and a rigid ring at the bottom. A rod running centrally from the top to the bottom carried a movable point gauge for measuring depths. A turntable fixed to the bottom ring supporting the transparent tube was driven by a variable-speed motor of 5 hp.

Water at 62°F was introduced into the tube through a rotating union threaded into the top hub from a head tank. The flow was regulated by needle valves through flow meters of the type of the Fischer–Porter rotometer. The flow meters were calibrated under test conditions and the variation of the discharge was within $\pm 1\%$ in each run. After entering the rotating union, the water was spread onto the inner wall of the best cylinder by a circular plate. Vertical uniform flow was established after approximately one tube diameter and a half.

At the bottom of the tube were efflux ports which could be opened or closed at will to adjust the location of the jump. The jump could be moved up the tube by reducing the opening at the bottom of the tube.

The angular speed of the turntable was measured electromagnetically and was maintained constant. The variation in each run was no more than 1 r.p.m., or about $\pm 0.1\%$ in the tests. This angular speed is the same as ω in the analysis. Figure 3 shows the location of the jump and streaks in the flow both upstream and downstream of the jump. Since ω was known and d_1 was small, the circumferential velocity upstream from the jump was known. Assuming the streaks were statistically the same as the streamlines, one could obtain the upstream surface velocity U_1 of the fluid in the axial direction from the inclination of the streaks.

[If the streaks are actually characteristics for surface waves, the effect of the assumption made here is to over-estimate U_1 and hence to underestimate d_1. In that case the experimental points in Fig. 4 should be shifted downward and to the right. The error introduced by the assumption would in that event increase with the speed of the surface waves, which in turn would depend on and probably increase with ω and d_1. If surface-wave speed greatly overshadows the actual speed of the fluid in determining the slope of the streaks, the streaks prior to the jump cannot be much steeper than those after it, since $d_2 > d_1$, and ω_2 is nearly equal to ω for the tests performed, according to (12). But the upstream streaks are much steeper than the downstream ones. Hence we believe the assumption made is not far wrong.]

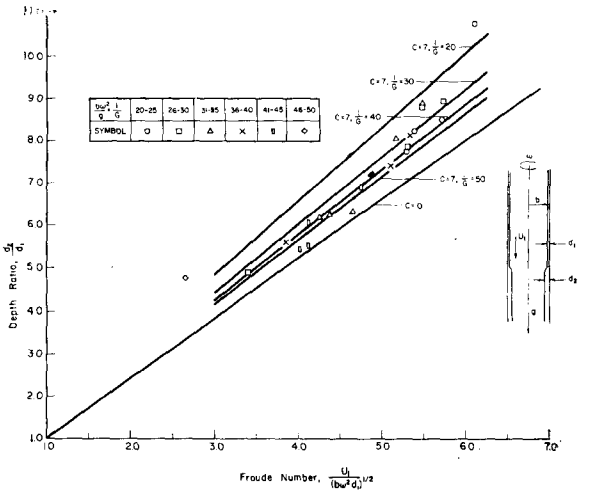

FIG. 4. Comparison of theoretical and experimental results.

From U_1 one can easily calculate d_1. The mean inclination of the streaks was obtained photographically with a variation of $\pm 0.5°$. Downstream from the jump the inclination of the streaks were too small to be useful as a reliable means of obtaining d_2, which was therefore measured with the point gauge. The error was approximately ± 0.007 in. The upstream depth was so small that the waviness of the free-surface would introduce a substantial percentage error in d_1 if measured with the point gauge. That was why the streaks were utilized upstream from the jump.

The length of the jump was observed to be between 0.5 and 1 in. in the tests.

4. DISCUSSION OF RESULTS

The results are shown in Table I and Fig. 4. As explained in Sec. 3, U_1 was computed from the inclination of the streaks on the upstream free surface. Since the upstream flow was assumed to be turbulent, this U_1 was considered to be the axial velocity in the major part of the upstream flow.

TABLE I. Data for rotating hydraulic jump.

Run	rpm	Q in.^{3}/sec	α deg	tan α	U_1 in./sec	d_1 in.	d_2 in.	F	$\frac{d_2}{d_1}$	R	$\frac{b\omega_1^2}{g}$
1	463	44.4	21.0	0.38	79	0.021	0.18	5.5	8.8	1400	25.8
2	535	42.2	19.8	0.36	86	0.018	0.16	5.5	8.9	1300	34.6
3	535	29.8	17.0	0.31	72	0.015	0.12	5.2	8.0	900	34.6
4	430	33.0	21.0	0.38	73	0.017	0.18	6.1	10.7	1000	22.4
5	540	44.4	19.7	0.36	86	0.019	0.16	5.3	8.1	1400	35.2
6	622	31.6	16.0	0.29	79	0.015	0.11	4.9	7.2	1000	47.1
7	592	32.8	16.3	0.29	77	0.016	0.11	4.7	6.9	1000	42.4
8	465	47.5	21.0	0.38	79	0.022	0.17	5.3	7.8	1500	26.2
9	565	47.5	18.8	0.34	86	0.021	0.15	4.9	7.2	1500	34.7
10	625	47.5	16.5	0.30	61	0.029	0.14	2.7	4.7	1500	47.2
11	455	53.3	23.0	0.42	86	0.023	0.21	5.7	9.2	1700	25.0
12	610	53.3	17.5	0.32	86	0.023	0.14	4.2	6.1	1700	45.0
13	550	53.3	20.2	0.37	90	0.022	0.16	5.1	7.4	1700	36.5
14	450	59.0	23.7	0.44	88	0.025	0.21	5.7	8.5	1900	24.5
15	525	59.0	20.0	0.36	85	0.026	0.16	4.6	6.3	1900	33.2
16	600	59.0	17.8	0.32	86	0.026	0.14	4.1	5.5	1900	43.6
17	450	64.2	23.5	0.43	87	0.028	0.23	5.4	8.2	2000	24.5
18	525	64.2	19.8	0.36	84	0.029	0.18	4.4	6.2	2000	33.2
19	600	64.2	18.0	0.32	87	0.028	0.15	4.0	5.4	2000	43.6
20	440	71.0	24.0	0.44	87	0.030	0.23	5.3	7.7	2200	23.6
21	525	71.0	20.0	0.36	85	0.031	0.19	4.3	6.1	2200	33.2
22	625	71.0	16.5	0.30	82	0.032	0.16	3.4	4.8	2200	47.2
23	575	76.2	18.7	0.34	87	0.033	0.18	3.8	5.6	2400	40.0

The Reynolds number

$$R = U_1 d_1/\nu$$

based on the surface velocity was recorded in Table I, with $\nu = 1.2 \times 10^{-5}$ ft^2/sec. The values of R show that the judgment of turbulent upstream flow is not an unrealistic one. It is known that plane Poiseuille flow, which would be the upstream flow if it were laminar and the slight curvature effect were neglected, is unstable at a value 2000 for the Reynolds member based on the mean velocity, or 3000 for R. It is also known that a free surface tends to destabilize the flow. But it is important to remember the distinction between stability against surface waves and that against shear waves. For surface waves the flow is unstable at any Reynolds number however small, but at the same time it is shear-wave instability that is responsible for turbulence. In view of the fact that the Reynolds numbers recorded are from 930 to 2400, which are of the order of 3000, and considering that the flow was not free from turbulence as it entered the tube, the assumption of turbulent upstream flow was not unrealistic. With Q as the discharge in cubic inches per second, d_1 was obtained from

$$d_1 = 0.0375\, Q/U_1,$$

U_1 being measured in inches per second.

In Fig. 4 the data are plotted in a chart with F as the abscissa and d_2/d_1 as the ordinate. Equation (19) is plotted with $c = 0$, and also, for best fit at various values of G, for $c = 7$. This value for c is the same as for the length of the ordinary hydraulic jump. It can be seen that the agreement between the theoretical prediction and the experimental results is quite satisfactory.

In none of the experiments did the tube run completely full of water downstream from the jump. Choking downstream from jump can happen if the discharge is great enough, or the pipe small enough, or the downstream opening narrow enough. If that happens, the situation is similar to the ordinary hydraulic jump when the water surface downstream touches an upper lid, the thin-film approximation is invalidated, and the radial variation of ω_2 is quite uncertain.